LCD with In-cell Integrated Temperature Sensors for Multi-Area Temperature Detection

Yuanyang Zhao, Xiaojie Zhang*, Hui Wang*, Sheng Wang*, Pengtao Li**, Xiaoxia Wang**, Jie Yu**, Rui Han***

* Hefei BOE Optoelectronic Technology Co., LTD. Hefei, China

** Beijing BOE Optoelectronic Technology Co., LTD. Beijing, China

Abstract

An integrated partitioned temperature sensing scheme within the panel is proposed to achieve temperature detection at any position on the panel. The effective display area is segmented into equal sub-areas, each equipped with a thermistor. Signals are gathered and processed by a dedicated Flexible Printed Circuit (FPC). The integrated thermal resistance wire, made panel-compatible, enables low-cost and high-precision temperature detection.

Author Keywords

Temperature sensor; Thermal resistance; Partition detection.

1. Introduction

The temperature monitoring of the screen has been put forward by some special use environment, such as the Vehicle HUD (Head-Up Display) system [1, 2]. Due to the influence of sunlight backflow, the display area of the screen will be irradiated by light spots of fixed size, causing a serious rise in local temperature, resulting in abnormal display or hardware damage. As shown in Figure 1, the rotable mirror used as the magnifying light path in the HUD usually adopts a concave mirror design, and the concave mirror also has the characteristics of optical focusing. When the PGU is illuminated by light spots, it could be disabled due to excessive temperature caused by the convergence of light, and even has the risk of PGU burn.

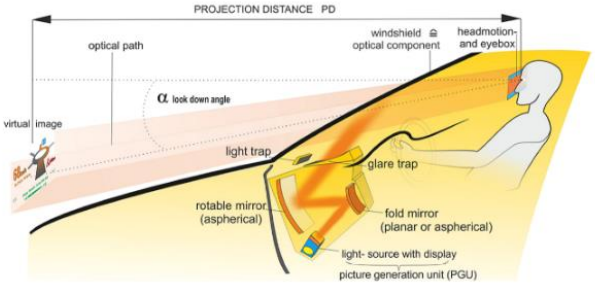

Figure 1. Working principle of Vehicle HUD system.

In view of this situation, if the detection area of the temperature sensor is not located in the light spot or it has not been integrated into the panel, the specific temperature in the light spot area cannot be accurately detected, resulting in identification errors.

This paper involves a panel scheme for areal temperature detection. The effective display area is divided into multiple sub-areas, the size of each sub-area matches the spot size of sunlight backfilling, and each sub-area is equipped with a separate metal thermistor coil [3, 4, 5] to monitor the temperature change in this area. Change of temperature at any position irradiated by the spot can be identified, thus achieving full coverage of panel temperature monitoring. As a result, it is convenient for the system to take cooling measures.

2. Panel design for temperature sensor

Sub-area Design: The temperature sensor was designed based on BOE 11.98-inch vehicle product. As shown in Figure 2 and Figure 3, it is divided into 150 sub-areas. Except for the irregular area, the remaining sub-areas are equal in size. Each sub-area is filled with metal coils, which are based on the principle of thermal resistance and react to changes in temperature through changes in resistance.

1	6	11	16	21	26	31	36	41	46	51	56	61	66	71	80	85	90	95	100	105	110	115	120	125	130	135	140	145	150
2	7	12	17	22	27	32	37	42	47	52	57	62	67	72	79	84	89	94	99	104	109	114	119	124	129	134	139	144	149
3	8	13	18	23	28	33	38	43	48	53	58	63	68	73	78	83	88	93	98	103	108	113	118	123	128	133	138	143	148
4	9	14	19	24	29	34	39	44	49	54	59	64	69	74	77	82	87	92	97	102	107	112	117	122	127	132	137	142	147
5	10	15	20	25	30	35	40	45	50	55	60	65	70	75	76	81	86	91	96	101	106	111	116	121	126	131	136	141	146

Figure 2. Panel design of 11.98 inch product.

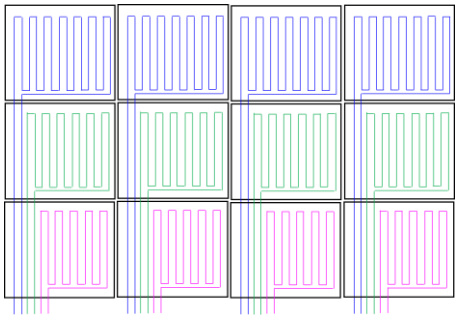

Figure 3. Detail diagram of sub-area.

Table 1 reveals the parameters of sensor design. Considering the accuracy of temperature detection, a complete sub-area should be contained in the spot irradiation area, thus the size of the sub-area should not be larger than the spot area. Based on the actual situation of the current vehicle HUD, we set the size of the sub-area to be about 10*10mm, which is equal to the size of the spot.

Table 1. Partition parameter

Item	11.98
Resolution	1500*256
Pixel Size(um)	200.08*200.1
Quantity of sensor	30*5
Sensor Pitch(Pixel)	50*50
Sensor Size(mm)	10.004*10.005

Pixel Design: Figure 4 reveals the pixel design scheme. The metal coil is located on the Array substrate and is compatible with the Array process. The pixel is equipped with a separate metal wire (purple) as the induction coil, which can be connected horizontally and vertically as required to achieve winding of the coil. In order to achieve this scheme, the process needs to be adjusted synchronously, we add a separate metal layer, and PVX is divided into PVX1 and PVX2 with double coating, but can be etched at one time. The metal layer is located between the SD layer and the ITO, while avoiding the pixel opening area. For the 11.98-inch product, the Dual Gate features allow for a vertical COM signal line separated from the Data, and a horizontal gap between the two Gate

ISSN 0097-996X/25/5603-1662-$1.00 © 2025

lines, both of which can be used to place induction coils without interfering with the display signal. As shown in the section diagram, the vertical induction line is located above the COM line and is covered by the COM ITO, which does not cause any change in the liquid crystal deflection, and the COM which as a DC signal does not cause coupling to the induction coil.

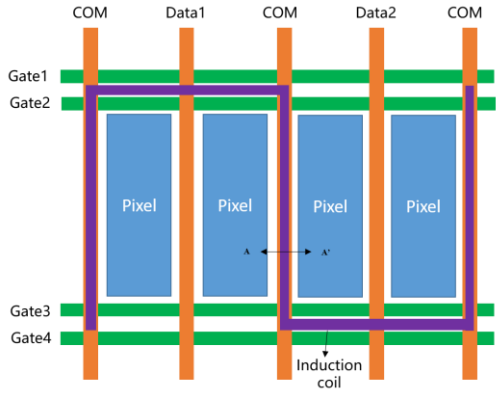

(a) Diagram of pixel design.

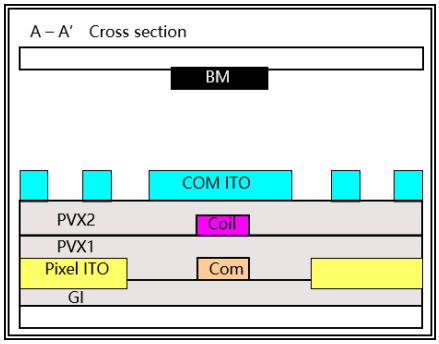

(b) Cross section of induction coil.

Figure 4. Pixel design and Section diagram.

Driving schemes: The coil is connected to the FPC terminal through the wire, and is connected to the MCU through the FPC. The MCU provides the detection signal to the coil and receives the feedback signal from the coil. When the light spot illuminates the sub-area, the temperature of the coil rises, and the resistance increases accordingly, resulting in the change of the accepted signal.

For the rectangular sub-area, the coil length of sub-area in same row is equal, the resistance is equal, and different rows of coil resistance will have a certain difference. In addition, there are some special-shaped sub-areas on the screen that are smaller than the rectangular area, and the coil resistance will also be different. However, the resistance value of the metal thermal resistance is basically linear with the temperature. Such as Al metal which used in this case, the TCR(Temperature Coefficient of Resistance) is about 0.42%/℃. Although there are differences in the resistance of different sub-areas, the ratio of temperature change is consistent, therefore a unified algorithm can be used to calculate the temperature change of all sub-areas. It is worth mentioning that, in addition to the linear calculation formula, the initial relationship of temperature and signal need to be calibrated and recorded. After the production of module, the screen is placed in a stable temperature environment, and the backlight and display can be turned off. After the screen reaches the presupposed temperature, the MCU monitors and records the corresponding data and temperature.

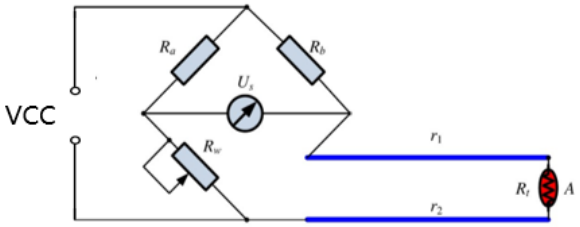

Figure 5. Wheatstone bridge circuit.

$$\Delta V = VCC \times \frac{R_b \cdot R_w - R_a \cdot R_t}{(R_a + R_w) \cdot (R_b + R_t)} \quad (1)$$

The algorithm of the signal amplification by Wheatstone bridge is shown in Figure 5 and formula (1). Since the coil resistance is large, about tens of thousands ohm, the amplification of the signal is necessary to ensure that the signal can be easily identified with the change of temperature.

For each sub-area, in addition to the detection coil inside the area, there is also a certain resistance in the external detection signal routing. If this part of the resistance is not taken into account, the resistance of the detection coil changes while the resistance of the routing remains unchanged when the light spot is irradiated on the partition, which will lead to unstable deviation of the detection results and affect the detection accuracy. Therefore, the ratio of routing resistance should be minimized in the design. At the same time, it is necessary to add some algorithm compensation for the resistance of this part. As shown in Figure 6, if the temperature of sub-area (1) is to be calculated, the total resistance and its change with temperature should be read out at the FPC end. The total resistance Rs1 consists of four parts, and the coil resistance Rc1 of sub-area (1) is included. The resistance of the wire (2) is Rw2; the resistance of the wire (3) is Rw3; the resistance of the wire (4) is Rw4. If the spot is illuminated in the sub-area (1), only Rc1 will change, and the resistance of the rest of the wire will be basically unchanged, so the result obtained according to the linear algorithm is not accurate. Consider the compensation algorithm, the calculation steps are as follows:

1. Coil (4) is set in area (4) to detect the temperature in area (4).
2. According to the temperature of area (4), the Rw4 corresponding to sub-area (3) is obtained, while the total resistance Rs3 of sub-area (3) is measured at the FPC end, and the coil resistance Rc3 of sub-area (3) is calculated according to formula 4. Finally, the temperature of sub-area (3) is obtained through the preset algorithm, that is, the temperature corresponding to the wiring (3).
3. According to the temperature of sub-area (3) calculated in the previous step, Rw3 is obtained; meanwhile, the total resistance Rs2 of sub-area (2) is measured at the FPC, and the coil resistance Rc2 of sub-area (2) is calculated according to formula 3. Finally, the temperature of sub-area (2) is obtained through the preset algorithm.
4. By analogy, the temperature of sub-area (1) is obtained according to formula (2).

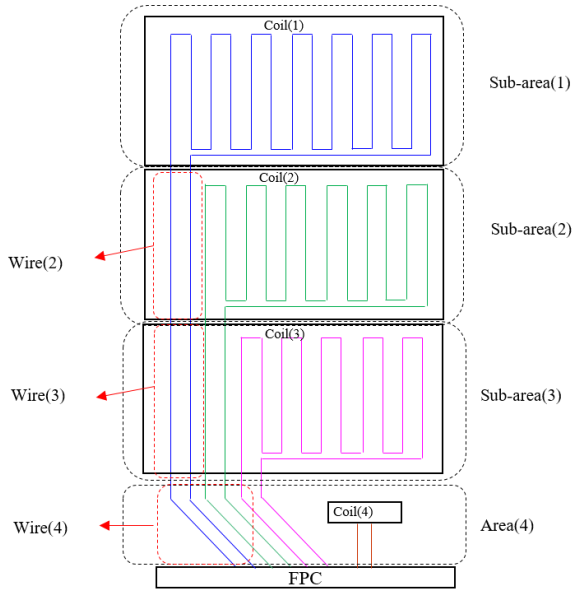

Figure 6. Algorithm compensation structure.

$$R_{s1}=R_{c1}+R_{w2}+R_{w3}+R_{w4} \quad (2)$$

$$R_{s2}=R_{c2}+R_{w3}+R_{w4} \quad (3)$$

$$R_{s3}=R_{c3}+R_{w4} \quad (4)$$

The compensation algorithm should be mentioned if the application scenario requires high accuracy of temperature detection, and the calculated temperature will not be affected by the routing resistance, and the accuracy is high.

Verification results: A complete 11.98-inch temperature sensing panel was produced through the above schemes. Based on the test results of the incubator, we obtained the core formula Y=0.0041x +1.128, where X is the temperature and Y is the resistance ratio of the corresponding temperature to the calibration point. The unified algorithm based on the core formula is applied to each sub-area in the panel. The test results are shown in Figure 7. The ordinate represents the measured temperature, and the abscissa represents 150 sub-areas, and the maximum test error between each sub-area does not exceed 1℃.

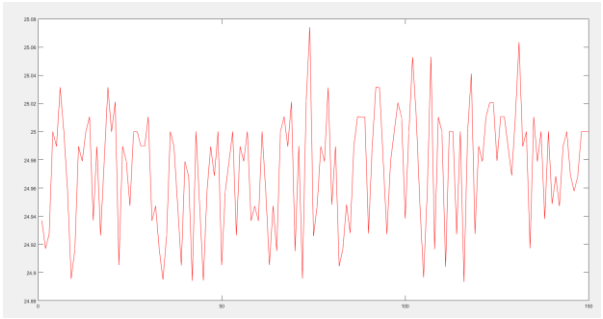

Figure 7. 25 ° C measurements in each sub-area.

We used a 10*10mm metal sheet which was heated by an electric soldering iron to simulate the heating effect of light spot irradiation. The test results are shown in Figure 8. After the metal sheet is placed, the temperature in the central sub-area rises to 79 °C.

46	41	43	39	44	41	41	41	47	45	46	49	44	49	43	42	45	40	41	47	44	46	43	44	42	47	51	48	42	43
39	38	38	46	41	47	44	47	43	42	40	42	42	44	42	42	42	48	46	44	44	49	46	47	49	47	42	44	43	46
40	47	44	43	44	43	42	43	45	48	45	40	46	43	47	46	48	46	41	45	48	43	46	42	42	42	46	43	47	40
44	39	44	40	45	39	45	48	47	40	43	47	43	44	42	39	43	41	47	42	43	45	42	46	46	46	42	42	40	44
37	41	42	45	40	45	40	40	41	46	47	43	42	46	41	44	46	44	43	47	45	45	42	43	42	45	43	48	42	46

(a) Temperature monitoring results before the metal sheet is placed.

45	41	43	39	44	40	40	41	47	45	45	49	43	50	44	43	45	39	41	48	44	46	41	43	41	47	50	48	41	45
38	38	37	46	40	47	44	47	41	41	39	42	46	54	45	43	40	47	47	43	44	48	46	47	49	47	41	43	42	46
39	46	43	42	44	42	41	41	44	47	45	41	63	79	57	48	47	45	41	44	50	43	46	40	42	41	46	41	48	40
45	39	43	39	44	38	45	47	46	39	43	50	49	59	46	39	41	40	47	42	42	44	42	46	46	46	41	41	39	44
37	41	41	46	40	46	40	39	40	46	47	42	42	47	42	45	46	46	42	47	44	45	42	44	41	45	42	48	42	47

(b) Temperature monitoring results after the metal sheet is placed.

Figure 8. Simulated spot exposure test.

The final temperature sensing panel is shown in Figure 9 with the overall system. In the upper right corner of the panel, the maximum temperature in the current panel and its corresponding position coordinate information are displayed.

Figure 9. Display effect of integrated panel.

3. Conclusion

In conclusion, this paper describes an 11.98-inch panel with regionalize temperature detection function. The display area is divided into several sub-areas, each sub-area is set with metal coil as temperature sensing unit. Based on the principle of metal thermal resistance, the signal strength changes of the metal coil in each area are detected, the changes of resistance value are calculated, and the temperature changes are finally obtained. We focus on its partition design, pixel design and driver scheme. This scheme solves the problem that the traditional temperature sensor can only detect the temperature of a small fixed area, and it cannot identify the panel burned by the sunlight on the vehicle HUD. It meets the needs of multi-point accurate detection. The metal coil is made through the Array process with low cost, and the metal thermal resistance is used to greatly reduce the impact of process fluctuations on the detection accuracy. In addition, the scheme

has simple structure and high compatibility, which can be extended to other types of display panels such as OLED, and can be applied to almost all display scenes with multi-point temperature monitoring.

4. References

1. Han H , Liu J , Xie X . An Analysis on HUD Technology in Navigation Field[J]. 2021.DOI:10.16661/j.cnki.1672-3791.2004-5311-1481.
2. Pang Y , Yumeng S , Chen T ,et al. Color holographic HUD with eyebox expansion using a folding optical path module[J]. 2022.DOI:10.1117/12.2643511.
3. Marangoni T A , Guralnik B , Borup K A ,et al.Determination of the temperature coefficient of resistance from micro four-point probe measurements[J].Journal of Applied Physics, 2021, 129(16):165105. DOI:10.1063/5.0046591.
4. Shin H , Duy L T , Seo H .Optimization of temperature coefficient of resistance of Al-doped vanadium oxide thin film prepared by atomic layer deposition for uncooled microbolometer[J].Ceramics International, 2022. DOI:10.1016/j.ceramint.2022.02.111.
5. Khan A I , Khakbaz P , Brenner K A ,et al.Large temperature coefficient of resistance in atomically thin two-dimensional semiconductors[J].Applied Physics Letters, 2020, 116(20):203105.DOI:10.1063/5.0003312.